MDPI

Article

Simple Levy-α stable model analysis of elastic pp and $p\bar{p}$ low-$|t|$ data from SPS to LHC energies

Tamás Csörgő [1,2], Sándor Hegyi [2] and István Szanyi [1,2,3,*]

[1] MATE Institute of Technology, Károly Róbert Campus, Mátrai út 36, H-3200 Gyöngyös, Hungary; tcsorgo@cern.ch
[2] Wigner Research Center for Physics, P.O. Box 49, H-1525 Budapest, Hungary; hegyi.physics@gmail.com
[3] Eötvös University, Department of Atomic Physics, Pázmány P. s. 1/A, H-1117 Budapest, Hungary
* Correspondence: iszanyi@cern.ch

Abstract: A simple Lévy-α stable (SL) model is used to describe the data on elastic pp and $p\bar{p}$ at low-$|t|$ from SPS energies up to LHC energies. The SL model is demonstrated to describe the data with a strong non-exponential feature in a statistically acceptable manner. The energy dependence of the parameters of the model is determined and analyzed. The Lévy α parameter of the model has an energy-independent value of 1.959 ± 0.002 following from the strong non-exponential behavior of the data. We strengthen the conclusion that the discrepancy between TOTEM and ATLAS elastic pp differential cross section measurements shows up only in the normalization and not in that shape of the distribution of the data as a function of t. The jump in the energy dependence of the slope parameter data around 3-4 GeV, as observed by the TOTEM Collaboartion, is seen also in the SL model analysis of the differential cross section data.

Keywords: elastic scattering; proton-proton; proton-antiproton; Lévy-α stable model.

1. Introduction

In a recent work [1], we formulated the real extended Levy-α stable generalized Bialas-Bzdak (LBB) model as the generalization of the Real extended Bialas-Bzdak (ReBB) model. In the latter model, the assumed quark and diquark constituents of the proton have Gaussian parton distributions and also the distance between these constituents has a Gaussian shape. The Gaussian distribution is the $\alpha = 2$ special case of the Levy-α stable distribution. The ReBB model gives a statistically acceptable description to the proton-proton (pp) and proton-antiproton ($p\bar{p}$) elastic scattering data in a limited kinematic range that does not include the low-$|t|$ domain characterized by a strong non-exponential shape. The LBB model with Levy-α stable parton and distance distributions may reproduce the strong non-exponential behavior seen in the low-$|t|$ data. To apply the full LBB model to analyze the data, however, we need to solve the problem of integrating products of two-dimensional Levy-α stable distributions, and access to relatively high computing resources is necessary. As a temporal solution, we introduced approximations that are valid at the low-$|t|$ domain of elastic scattering lading to a simple Levy-α stable (SL) model [1]. We demonstrated that the SL model describes the non-exponential low-$|t|$ differential cross section of pp scattering at 8 TeV in a statistically acceptable manner. The ReBB model does not reproduce this strong non-exponential feature of the data.

The SL model gives the following shape to the elastic differential cross section:

$$\frac{\mathrm{d}\sigma}{\mathrm{d}t}(s,t) = a(s)e^{-|tb(s)|^{\alpha_L(s)/2}}, \tag{1}$$

where α_L, a, and b are fit parameters to be determined at a given energy. The parameter a is called the optical point as this is the value of the differential cross section at $t = 0$. The parameter is the Levy slope parameter and α_L is the Levy α parameter. The $\alpha_L = 2$

Citation: Csörgő, T.; Hegyi, S; Szanyi, I. Title Citation to fill. *Universe* **2023**, *1*, 0. https://doi.org/

Received:
Accepted:
Published:

cease corresponds to a Gaussian impact parameter profile and an exponential differential cross section. In case $0 < \alpha_L < 2$, the impact parameter profile is Levy-α stable distributed having a long tale and the differential cross section is non-exponential as a function of t.

In the framework of the Regge approach, the non-exponential behavior of the elastic differential cross section at ISR [2–4] and later also at TEVATRON and LHC [5–10] was related to the $4m_\pi^2$ branch point of t-channel scattering amplitude and hence is explained as the manifestation of t-channel unitarity. According to the findings of Refs. [11,12] the low-$|t|$ non-exponential behavior of elastic pp differential cross-section can be a consequence of an interplay between the real parts of the Coulomb and nuclear amplitudes.

In this work we use the SL model as defined by Eq. (1) to analyze the low-$|t|$ pp and $p\bar{p}$ elastic scattering data in the energy range that includes SPS and LHC energies. The details and results of the fits are presented in Sec. 2. The energy dependence of the parameters of the model is determined in Sec. 3. The results are discussed in Sec. 4 and summarized in Sec. 5.

2. Fits

The fitting procedure was performed by using a χ^2 definition which relies on a method developed by the PHENIX Collaboration [13]. This χ^2 definition is equivalent to the diagonalization of the covariance matrix of statistical and systematic uncertainties if the experimental errors are separated into three different types:

- type a: point-to-point varying uncorrelated systematic and statistical errors;
- type b: point-to-point varying and 100% correlated systematic errors;
- type c: point-independent, overall correlated systematic uncertainties, that scale all the data points up and down by the same factor.

We categorized the available experimental uncertainties into these three types as follows: horizontal and vertical t-dependent statistical errors (type a), horizontal and vertical t-dependent systematic errors (type b), and overall normalization uncertainties (type c). The χ^2 function used in the fitting procedure is:

$$\chi^2 = \left(\sum_{i=1}^{N} \frac{(d_i + \epsilon_b \widetilde{\sigma}_{bi} + \epsilon_c \sigma_c d_i - m_i)^2}{\widetilde{\sigma}_i^2} \right) + \epsilon_b^2 + \epsilon_c^2, \tag{2}$$

where

$$\widetilde{\sigma}_i^2 = \widetilde{\sigma}_{ai} \left(\frac{d_i + \epsilon_b \widetilde{\sigma}_{bi} + \epsilon_c \sigma_c d_i}{d_i} \right), \tag{3}$$

$$\widetilde{\sigma}_{ki} = \sqrt{\sigma_{ki}^2 + (d_i' \delta_k t_i)^2}, \;\; k \in \{a, b\}, \;\; d'(t_i) = \frac{d_{i+1} - d_i}{t_{i+1} - t_i}, \tag{4}$$

N is the number of fitted data points, d_i is the ith measured data point and m_i is the corresponding value calculated from the model; σ_{ki} is the type $k \in \{a, b\}$ error of the data point i, σ_c is the type c overall error given in percents, d'_{ij} denotes the numerical derivative in point t_i with errors of type $k \in \{a, b\}$, denoted as $\delta_k t_i$; ϵ_l is the correlation coefficient for type $l \in \{b, c\}$ error. These correlation coefficients are fitted to the data and must be considered as both free parameters and data points not altering the number of degrees of freedom. The χ^2 definition, Eq. (2), was utilized and further detailed in Ref. [14].

The SL model was fitted using the above detailed χ^2 definition, Eq. (2), to all the available pp and $p\bar{p}$ differential cross-section data in the kinematic range of 0.546 TeV $\leq \sqrt{s} \leq$ 13 TeV and 0.02 GeV$^2 \leq -t \leq$ 0.15 GeV^2. This means 11 different data sets. The values of the parameters of the model at different energies as well as the confidence levels of the fits and the data sources are shown in Table 1. One can see that the confidence level (CL) values range from 8.8% to 96% implying that the SL model represents the data in a statistically acceptable manner. We regard a fit by a model to be a statistically acceptable description in case 0.1 % $\leq$ CL $<$ 99.9 %.

$\sqrt{s}$ [GeV]	data from	α_L	a [mb/GeV^2]	b [GeV^{-2}]	CL (%)
546	UA4 [15]	1.93 ± 0.09	209 ± 15	15.8 ± 0.9	18.1
1800	E-710 [16]	2.0 ± 1.5	270 ± 24	16.2 ± 0.2	77.1
2760	TOTEM [17]	1.6 ± 0.3	637 ± 25	28 ± 11	20.5
7000	TOTEM [18]	1.95 ± 0.01	535 ± 30	20.5 ± 0.2	8.8
7000	ATLAS [19]	1.97 ± 0.01	463 ± 13	19.8 ± 0.2	96.0
8000	TOTEM [20]	1.955 ± 0.005	566 ± 31	20.09 ± 0.08	43.9
8000	TOTEM [21]	1.90 ± 0.03	582 ± 33	20.9 ± 0.4	19.6
8000	ATLAS [22]	1.97 ± 0.01	480 ± 11	19.9 ± 0.1	55.8
13000	TOTEM [23]	1.959 ± 0.006	677 ± 36	20.99 ± 0.08	76.5
13000	TOTEM [24]	1.958 ± 0.003	648 ± 95	21.06 ± 0.05	89.1
13000	ATLAS [25]	1.968 ± 0.006	569 ± 17	20.84 ± 0.07	29.7

Table 1. The values of the parameters of the SL model at different energies from half TeV up to 13 TeV. The last column shows the confidence level of the fit to that date at different energies.

3. Energy dependence

Using the values of the parameters of the model at different energies given in Tab. 1, we determined the energy dependence of these parameters.

Table 1 indicates that the TOTEM datasets at $\sqrt{s} = 2.76$, 7, 8 and 13 TeV, as well as the ATLAS dataset at $\sqrt{s} = 2.76$ feature a strongly non-exponential shape with α_L significantly less than 2. The other datasets provide a less precise value for this Levy exponent.

The $\alpha_L(s)$ parameters can be fitted with an energy independent constant α_L value, as shown in Fig. 1. This average, constant value of the α_L parameter is consistent with all the measurements, with $\alpha_L = 1.959 \pm 0.002$. Although this average value is close to the Gaussian $\alpha_L = 2$ case, that corresponds to an exponentially shaped cone of the differential cross section of elastic scattering, its error is small and thus the constant value of is α_L significantly less than 2, indicating that a strongly non-exponential SL model is consistent with all the datasets shown in Table 1.

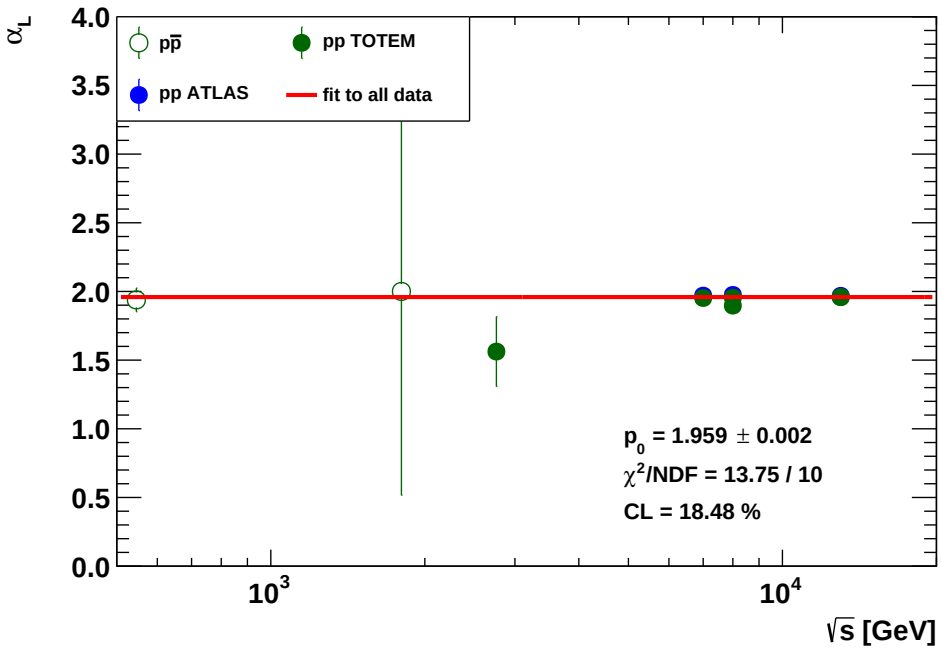

Figure 1. The values of the α_L parameter of the SL model at different energies from half TeV up to 13 TeV. The α_L parameter of the model is energy independent: its values at different energies can be fitted with a constant, 1.959 ± 0.002.

The energy dependence of the optical parameter a is shown in Fig. 2. For $p\bar{p}$ and ATLAS or $p\bar{p}$ and TOTEM data in the energy rangy range 0.546 TeV $\leq \sqrt{s} \leq$ 13 TeV the energy dependence of the a parameter is compatible with a quadratically logarithmic shape,

$$a(s) = p_0 + p_1 \ln\Big(\frac{s}{1\ \mathrm{GeV}^2}\Big) + p_2 \ln^2\Big(\frac{s}{1\ \mathrm{GeV}^2}\Big). \tag{5}$$

For $p\bar{p}$ and ATLAS data the values of the parameters in Eq. (5) are $p_0 = 1213 \pm 604$ mb/GeV^2, $p_1 = -180 \pm 79$ mb/GeV^2, and $p_2 = 8 \pm 2$ mb/GeV^2 resulting a confidence level of 33.22 %. For $p\bar{p}$ and TOTEM data the parameter values are $p_0 = 1133 \pm 523$ mb/GeV^2, $p_1 = -161 \pm 69$ mb/GeV^2, and $p_2 = 7 \pm 2$ mb/GeV^2 resulting a confidence level of 82.30 %. A fit by the parametrization Eq. (5) that includes a parameter values for all data – $p\bar{p}$, ATLAS, and TOTEM – is statistically not acceptable since its confidence level is 6.06 $\times$ 10^{-4} %.

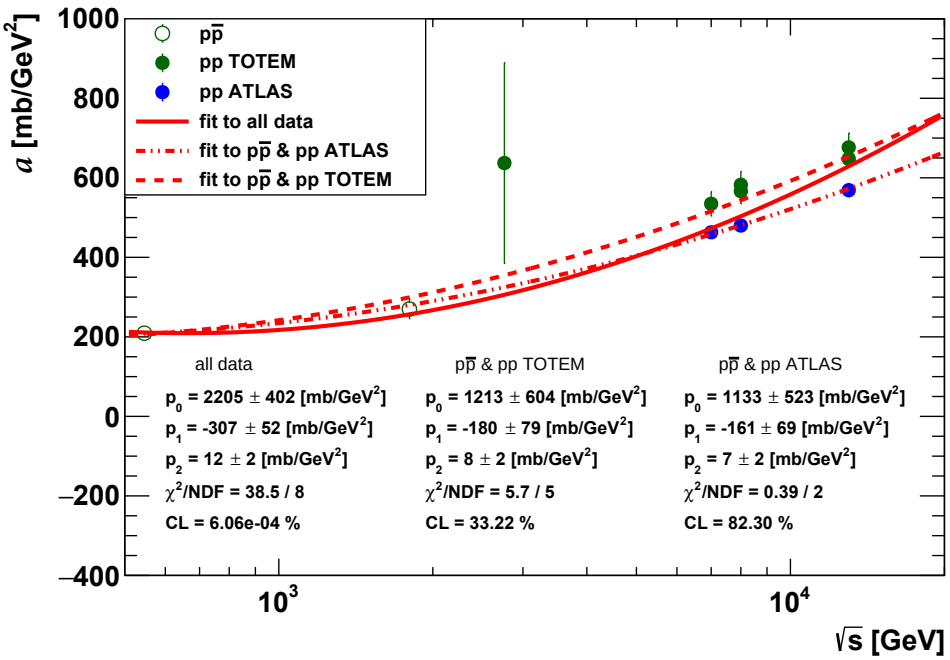

Figure 2. The values of the optical point parameter of the SL model at different energies from half TeV up to 13 TeV.

The energy dependence of the slope parameter b is shown in Fig. 3. For ATLAS or TOTEM pp data the energy dependence of the b parameter is compatible with a linearly logarithmic shape,

$$b(s) = p_0 + p_1 \ln\Big(\frac{s}{1\ \mathrm{GeV}^2}\Big), \tag{6}$$

with $p_0 = 4 \pm 1$ GeV^{-2} and $p_1 = 0.88 \pm 0.07$ GeV^{-2} resulting a confidence level of 0.36%. This result, illustrated in Fig. 3, when taken together with the results of Figs. 1 and 2, suggests that ATLAS and TOTEM data in the low $-t$ region have a consistent non-exponential shape, but differ in their overall normalization.

The values of the b parameter for $p\bar{p}$ data lie on the line given by Eq. (6) with parameters $p_0 = 14 \pm 6$ GeV^{-2} and $p_1 = 0.2 \pm 0.4$ GeV^{-2}. These values are significantly different from the values of linearity for elastic pp collisions. A fit by the parametrization Eq. (5) that includes b parameter values for all data – $p\bar{p}$, ATLAS, and TOTEM – is statistically not acceptable as it has too small a confidence level of 1.45×10^{-3} %.

4. Discussion

In this work we fitted the low-$|t|$ elastic pp and $p\bar{p}$ differential cross section in the center of mass energy range 0.546 TeV $\leq \sqrt{s} \leq$ 13 TeV. To do this we used the SL model as defined

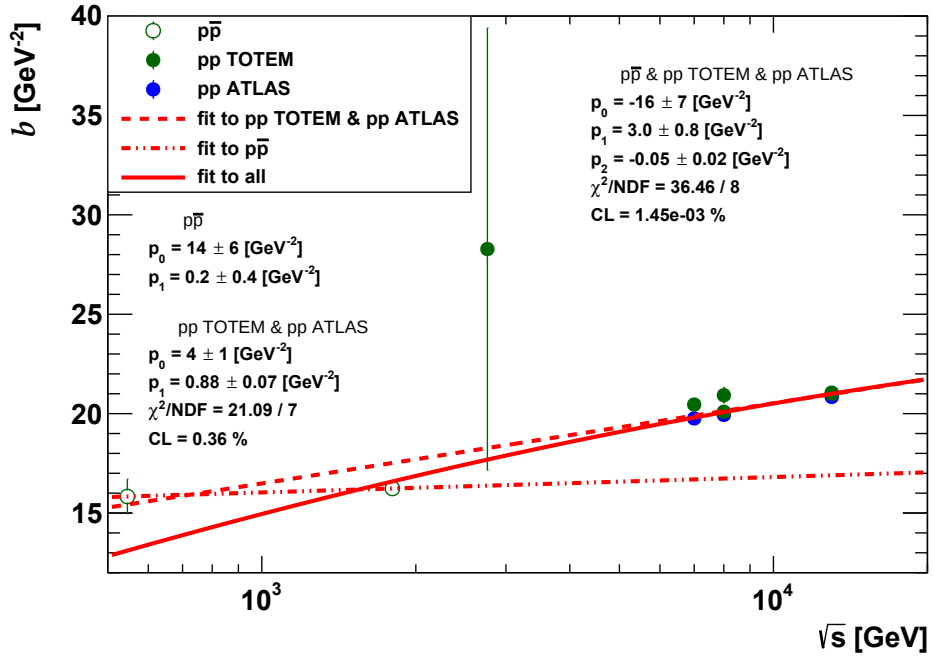

Figure 3. The values of the slope parameter of the SL model at different energies from half TeV to 13 up TeV.

by Eq. (1). Another popular empirical parametrisation for the low-$|t|$ non-exponential differential cross section is [1,20]

$$\frac{d\sigma}{dt} = \tilde{a}e^{-\tilde{b}t+\tilde{c}t^2}, \tag{7}$$

where $\tilde{a}$ is the optical point parameter, $\tilde{b}$ is the slope parameter, and $\tilde{c}$ is the curvature parameter. The tilde is to distinguish between the parameters in the SL model, Eq. (1), and in the model given by Eq. (7). The effect of the quadratic term in the exponent of Eq. (7) is reproduced in our model by an α_L parameter value less than 2.

An exponential differential cross section corresponds to a Gaussian impact parameter profile. The Gaussian distribution is the $\alpha_L = 2$ special case of the more general Lévy-α stable distributions. The experimentally observed non-exponetial differential cross section indicates that the impact parameter profile rather has a Lévy-α stable shape resulting the SL model given by Eq. (1). Accordingly, it may be more natural to use Eq. (1) instead of Eq. (7) to model the experimental data.

As an illustrative example, the SL model fit to the most precise TOTEM data measured at $\sqrt{s} = 13$ TeV [24] is shown in Fig. 4 and the case with $\alpha_L = 2$ fixed is shown in Fig. 5. The SL model with $\alpha_L = 1.958 \pm 0.003$ describes the 13 TeV TOTEM data with CL = 89.12 % while the $\alpha_L = 2$ fixed case fit has a confidence level of 3.6×10^{-27} %. These values are not surprising if one compares the bottom panel of Fig. 4 to the bottom panel of Fig. 5. This result clearly shows the need for an α_L parameter value slightly but in a statistical sense significantly less than 2.

Looking at the bottom panel of Fig. 4 one can observe some oscillations in the data. This oscillation is a significant effect when only the statistical errors are considered. If systematic errors are taken into account too, this oscillation effect disappeares. This conclusion is clear from the confidence level of the description by the SL model that does not have an oscillatory shape.

Let us now discuss the energy dependence of the SL model parameters.

According to our analysis, surprisingly, the α_L parameter of the SL model is energy-independent and its value is slightly but in a statistical sense significantly less than 2 implying a Lévy-α-stable-shaped, power-law tail feature for impact parameter profile of elastic pp and $p\bar{p}$ scattering.

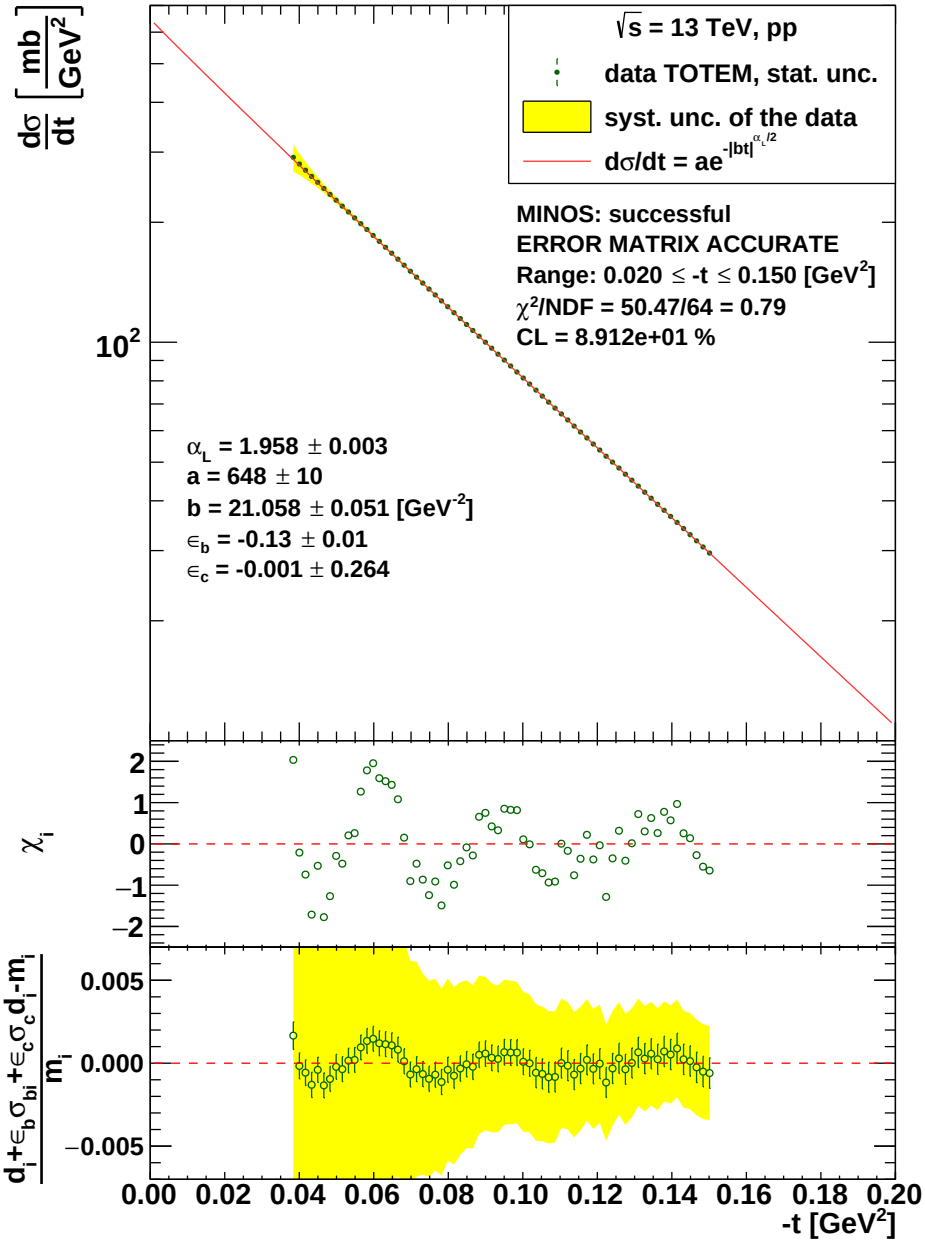

Figure 4. Fit to the low-$|t|$ pp differential cross section data measured by TOTEM at $\sqrt{s} = 13$ TeV [24] with the SL model defined by Eq. (1). The differential cross section data with the fitted model curve as well as the values of the fit parameters and the fit statistics are shown in the top panel. The middle panel shows the χ value contribution of the data points. The bottom panel shows the deviation of the $d\sigma/dt$ data points shifted within errors by the correlation parameters of the χ^2 definition Eq. (2) from the $d\sigma/dt$ calculated from the model relative to the $d\sigma/dt$ calculated from the model.

We showed in Sec. 3 that the energy dependence of the optical point parameter of the SL model is compatible with a quadratically logarithmic shape, however, the a parameter values determined from ATLAS and TOTEM data on pp elastic scattering disagree. This discrepancy is a well-known fact and the interpretation is that the ATLAS and TOTEM experiments use different methods to obtain the absolute normalization of the measurements [25].

In Ref. [1], we discussed that the optical point parameter is related to the α or opacity parameter of the LBB model which regulates the magnitude of the real size of the elastic

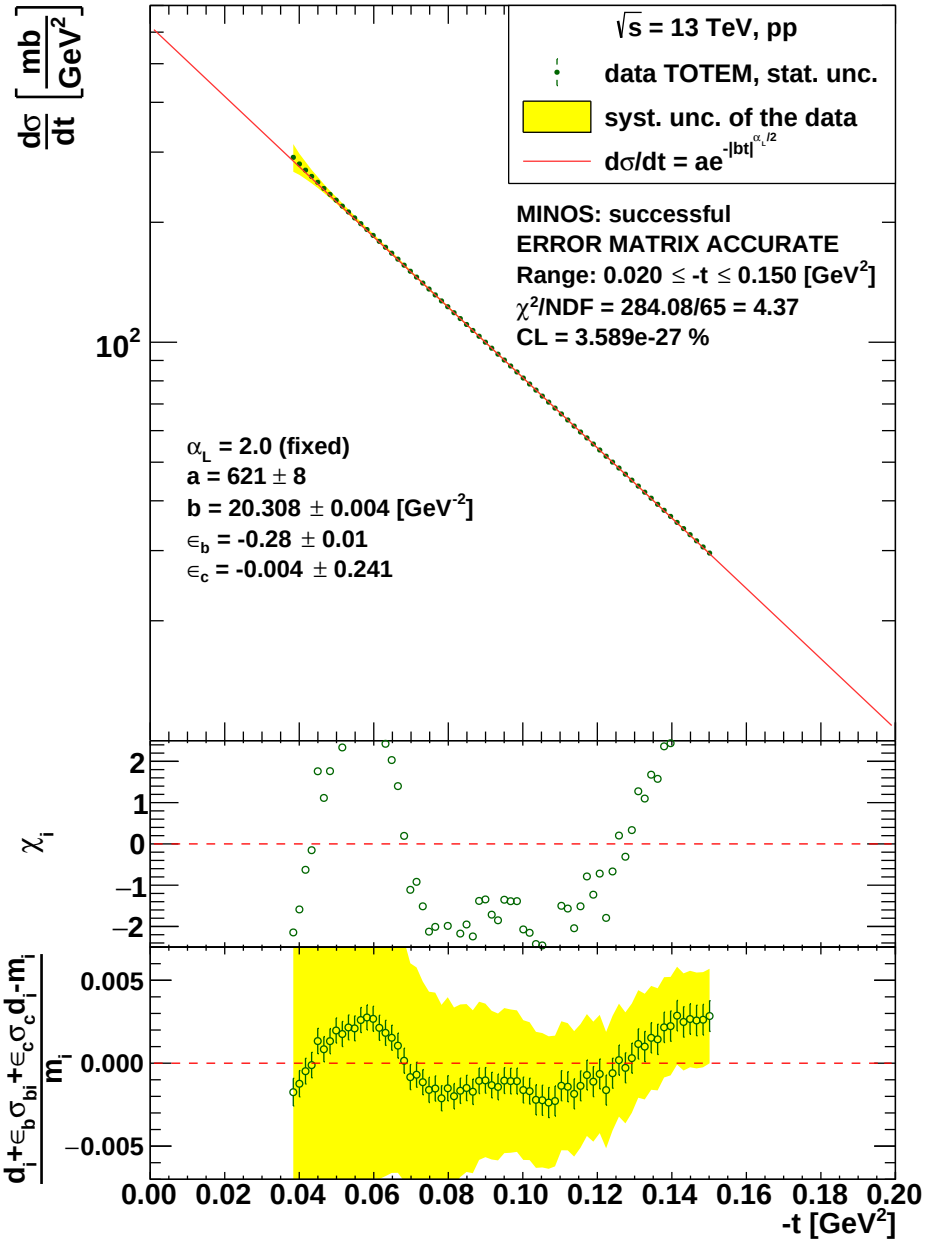

Figure 5. Same as Fig. 1 but with $\alpha_L = 2$ fixed.

scattering amplitude. Note that this opacity parameter α is not to be confused with the Levy index of stability α_L, where the subscript $_L$ stands for Lévy. The value of the opacity parameter α is different in pp and $p\bar{p}$ elastic scattering at the same energies. This implies different values for pp and $p\bar{p}$ optical points too. Such a conclusion is seemingly in disagreement with the result of Sec. 3 that $p\bar{p}$ and pp a parameter values lie in the same curve. There is no real contradiction, only the precision of the measurements is too low to see the difference between pp and $p\bar{p}$ optical points experimentally.

According to our results presented in Ref. [1], the slope parameter of the SL model can be written in terms of the parameters of the LBB model that have the same values in pp and $p\bar{p}$ elastic scattering at the same energies. This implies that slope parameters extracted from pp and $p\bar{p}$ data should lie in the same energy dependence curve. Such a conclusion is again seemingly in disagreement with the result of Sec. 3. We saw in Sec. 3 that pp and $p\bar{p}$ b parameter values lie in different curves. There is no real contradiction again. The TOTEM

Collaboration discussed in Ref. [26] that there is a jump in the energy dependence of the slope parameter in the energy interval of 3 GeV $\lesssim \sqrt{s} \lesssim$ 4 GeV. This jump is seen in our analysis too, preventing the lower energy $p\bar{p}$ data to lie in the same curve with the higher energy LHC ATLAS and TOTEM data.

5. Summary

We fitted the pp and $p\bar{p}$ elastic differential cross section with a simple Lévy-α stable model in the center of mass energy range 0.546 TeV $\leq \sqrt{s} \leq$ 13 TeV and in the four-momentum transfer range 0.02 GeV$^2 \leq -t \leq$ 0.15 GeV^2. We determined the energy dependence of the three parameters of the model. The Lévy index of stability, $\alpha_L(s)$ results are consistent with an energy independent, constant value, that is slightly but significantly smaller than 2. The energy dependence of the optical point parameter is the same for pp and $p\bar{p}$ processes and has a quadratically logarithmic shape, however, because of normalization differences, TOTEM and ATLAS optical point data are not the same within experimental errors and thus they can be fitted separately from one another but both can be fitted together with $p\bar{p}$ data. In our Lévy analysis the we observe the "jumping" behavior in the energy dependence of the Lévy slope parameter $b(s)$ in the energy interval of 3 GeV $\lesssim \sqrt{s} \lesssim$ 4 GeV as discussed by TOTEM in Ref. [26]. We also find that TOTEM and ATLAS slope parameter data can be fitted together with a linearly logarithmic shape indicating that TOTEM and ATLAS data different only in their normalization, but their shape is consistent. Similar conclusions were drawn in Ref. [27] concerning the TOTEM-ATLAS discrepancy at 13 TeV.

Acknowledgments: We greatfully acknowledge inspiring discussions with A. Ster and V. Petrov and the support from NKFIH Grants no. K133046, K147557 and 2020-2.2.1-ED-2021-00181; MATE KKP 2023; ÚNKP-23-3 New National Excellence Program of the Ministry for Culture and Innovation from the source of the National Research, Development and Innovation Fund.

Author Contributions: Conceptualization, T.C.; methodology, T.C., S.H., and I.S.; investigation, I.S.; writing—original draft preparation, I.S.; writing—review and editing, T.C. and S.H.; supervision, T.C. All authors have read and agreed to the published version of the manuscript.

Funding: NKFIH Grants no. K133046, K147557 and 2020-2.2.1-ED-2021-00181; MATE KKP 2023; ÚNKP-23-3 New National Excellence Program of the Ministry for Culture and Innovation from the source of the National Research, Development and Innovation Fund.

Institutional Review Board Statement: Not applicable.

Informed Consent Statement: Not applicable.

Conflicts of Interest: The authors declare no conflict of interest.

References

1. Csörgő, T.; Hegyi, S.; Szanyi, I. Lévy α-Stable Model for the Non-Exponential Low-|t| Proton–Proton Differential Cross-Section. *Universe* **2023**, *9*, 361, [arXiv:hep-ph/2308.05000]. https://doi.org/10.3390/universe9080361.
2. Cohen-Tannoudji, G.; Ilyin, V.V.; Jenkovszky, L.L. A model for the pomeron trajectory. *Lett. Nuovo Cim.* **1972**, *5S2*, 957–962. https://doi.org/10.1007/BF02777999.
3. Anselm, A.A.; Gribov, V.N. Zero pion mass limit in interactions at very high-energies. *Phys. Lett. B* **1972**, *40*, 487–490. https://doi.org/10.1016/0370-2693(72)90559-X.
4. Tan, C.I.; Tow, D.M. Can Pions Be the Dominant Linkage in Multiperipheral Cluster Models? *Phys. Lett. B* **1975**, *53*, 452–456. https://doi.org/10.1016/0370-2693(75)90216-6.
5. Khoze, V.A.; Martin, A.D.; Ryskin, M.G. Soft diffraction and the elastic slope at Tevatron and LHC energies: A MultiPomeron approach. *Eur. Phys. J. C* **2000**, *18*, 167–179, [hep-ph/0007359]. https://doi.org/10.1007/s100520000494.
6. Jenkovszky, L.; Lengyel, A. Low-|t| structures in elastic scattering at the LHC. *Acta Phys. Polon. B* **2015**, *46*, 863–878, [arXiv:hep-ph/1410.4106]. https://doi.org/10.5506/APhysPolB.46.863.
7. Fagundes, D.A.; Jenkovszky, L.; Miranda, E.Q.; Pancheri, G.; Silva, P.V.R.G. Fine structure of the diffraction cone: from ISR to the LHC. In Proceedings of the Gribov-85 Memorial Workshop on Theoretical Physics of XXI Century, 9 2015, [arXiv:hep-ph/1509.02197]. https://doi.org/10.1142/9789813141704_0022.

8. Jenkovszky, L.; Szanyi, I. Fine structure of the diffraction cone: manifestation of t channel unitarity. *Phys. Part. Nucl. Lett.* **2017**, *14*, 687–697, [arXiv:hep-ph/1701.01269]. https://doi.org/10.1134/S1547477117050065.
9. Jenkovszky, L.; Szanyi, I. Structures in the diffraction cone: The "break" and "dip" in high-energy proton–proton scattering. *Mod. Phys. Lett. A* **2017**, *32*, 1750116, [arXiv:hep-ph/1705.04880]. https://doi.org/10.1142/S0217732317501164.
10. Jenkovszky, L.; Szanyi, I.; Tan, C.I. Shape of Proton and the Pion Cloud. *Eur. Phys. J. A* **2018**, *54*, 116, [arXiv:hep-ph/1710.10594]. https://doi.org/10.1140/epja/i2018-12567-5.
11. Kohara, A.K. Forward scattering amplitudes of pp and $p\bar{p}$ with crossing symmetry and scaling properties. *J. Phys. G* **2019**, *46*, 125001, [arXiv:hep-ph/1906.01402]. https://doi.org/10.1088/1361-6471/ab47d3.
12. Kohara, A.K.; Ferreira, E.; Rangel, M. The interplay of hadronic amplitudes and Coulomb phase in LHC measurements at 13 TeV. *Phys. Lett. B* **2019**, *789*, 1–6, [arXiv:hep-ph/1811.03212]. https://doi.org/10.1016/j.physletb.2018.12.021.
13. Adare, A.; et al. Quantitative Constraints on the Opacity of Hot Partonic Matter from Semi-Inclusive Single High Transverse Momentum Pion Suppression in Au+Au collisions at s(NN)**(1/2) = 200-GeV. *Phys. Rev.* **2008**, *C77*, 064907, [arXiv:nucl-ex/0801.1665]. https://doi.org/10.1103/PhysRevC.77.064907.
14. Csörgő, T.; Szanyi, I. Observation of Odderon effects at LHC energies: a real extended Bialas–Bzdak model study. *Eur. Phys. J. C* **2021**, *81*, 611, [arXiv:hep-ph/2005.14319]. https://doi.org/10.1140/epjc/s10052-021-09381-5.
15. Battiston, R.; et al. Proton - Anti-proton Elastic Scattering at Four Momentum Transfer Up to 0.5-GeV**2 at the CERN SPS Collider. *Phys. Lett. B* **1983**, *127*, 472. https://doi.org/10.1016/0370-2693(83)90296-4.
16. Amos, N.A.; et al. $\bar{p}p$ Elastic Scattering at $\sqrt{s}$ = 1.8-TeV from $|t| = 0.034 - GeV/c^2$ to $0.65 - GeV/c^2$. *Phys. Lett. B* **1990**, *247*, 127–130. https://doi.org/10.1016/0370-2693(90)91060-O.
17. Antchev, G.; et al. Elastic differential cross-section $d\sigma/dt$ at $\sqrt{s} = 2.76$ TeV and implications on the existence of a colourless C-odd three-gluon compound state. *Eur. Phys. J.* **2020**, *C80*, 91, [arXiv:hep-ex/1812.08610]. https://doi.org/10.1140/epjc/s10052-020-7654-y.
18. Antchev, G.; et al. Measurement of proton-proton elastic scattering and total cross-section at $\sqrt{s}$ = 7 TeV. *EPL* **2013**, *101*, 21002. https://doi.org/10.1209/0295-5075/101/21002.
19. Aad, G.; et al. Measurement of the total cross section from elastic scattering in pp collisions at $\sqrt{s} = 7$ TeV with the ATLAS detector. *Nucl. Phys. B* **2014**, *889*, 486–548, [arXiv:hep-ex/1408.5778]. https://doi.org/10.1016/j.nuclphysb.2014.10.019.
20. Antchev, G.; et al. Evidence for non-exponential elastic proton–proton differential cross-section at low $|t|$ and $\sqrt{s}$ = 8 TeV by TOTEM. *Nucl. Phys.* **2015**, *B899*, 527–546, [arXiv:hep-ex/1503.08111]. https://doi.org/10.1016/j.nuclphysb.2015.08.010.
21. Antchev, G.; et al. Measurement of elastic pp scattering at $\sqrt{s} = 8$ TeV in the Coulomb–nuclear interference region: determination of the ρ-parameter and the total cross-section. *Eur. Phys. J.* **2016**, *C76*, 661, [arXiv:nucl-ex/1610.00603]. https://doi.org/10.1140/epjc/s10052-016-4399-8.
22. Aaboud, M.; et al. Measurement of the total cross section from elastic scattering in pp collisions at $\sqrt{s} = 8$ TeV with the ATLAS detector. *Phys. Lett. B* **2016**, *761*, 158–178, [arXiv:hep-ex/1607.06605]. https://doi.org/10.1016/j.physletb.2016.08.020.
23. Antchev, G.; et al. First determination of the ρ parameter at $\sqrt{s} = 13$ TeV: probing the existence of a colourless C-odd three-gluon compound state. *Eur. Phys. J.* **2019**, *C79*, 785, [arXiv:hep-ex/1812.04732]. https://doi.org/10.1140/epjc/s10052-019-7223-4.
24. Antchev, G.; et al. Elastic differential cross-section measurement at $\sqrt{s} = 13$ TeV by TOTEM. *Eur. Phys. J. C* **2019**, *79*, 861, [arXiv:hep-ex/1812.08283]. https://doi.org/10.1140/epjc/s10052-019-7346-7.
25. Aad, G.; et al. Measurement of the total cross section and ρ-parameter from elastic scattering in pp collisions at $\sqrt{s} = 13$ TeV with the ATLAS detector. *Eur. Phys. J. C* **2023**, *83*, 441, [arXiv:hep-ex/2207.12246]. https://doi.org/10.1140/epjc/s10052-023-11436-8.
26. Antchev, G.; et al. First measurement of elastic, inelastic and total cross-section at $\sqrt{s} = 13$ TeV by TOTEM and overview of cross-section data at LHC energies. *Eur. Phys. J. C* **2019**, *79*, 103, [arXiv:hep-ex/1712.06153]. https://doi.org/10.1140/epjc/s10052-019-6567-0.
27. Petrov, V.A.; Tkachenko, N.P. ATLAS vs TOTEM: Disturbing Divergence **2023**. [arXiv:hep-ph/2303.01058].